



ELSEVIER

Available online at [www.sciencedirect.com](http://www.sciencedirect.com)

Icarus ●●● (●●●●) ●●●-●●●

ICARUS

[www.elsevier.com/locate/icarus](http://www.elsevier.com/locate/icarus)

Note

# Sea-surface wave growth under extraterrestrial atmospheres. Preliminary wind tunnel experiments with application to Mars and Titan

Ralph D. Lorenz<sup>a,\*</sup>, Erin R. Kraal<sup>b</sup>, Eric E. Eddlemon<sup>c,d</sup>, Jered Cheney<sup>c,d,1</sup>, Ronald Greeley<sup>c</sup><sup>a</sup> Lunar and Planetary Laboratory, University of Arizona, Tucson, AZ 85721, USA<sup>b</sup> Earth and Planetary Sciences, University of California, Santa Cruz, CA 95064, USA<sup>c</sup> Department of Geological Sciences, Arizona State University, Tempe, AZ 85287, USA<sup>d</sup> NASA Ames Research Center, MS 242-6, Moffett Field, CA 94035, USA

Received 12 December 2003; revised 22 November 2004

## Abstract

We describe for the first time the generation and measurement of capillary waves in a water surface in a wind tunnel running with air at pressures of 15–1000 mbar. These experiments suggest a stronger dependence of wave generation on atmospheric density than the simple proportionality that might be expected from energy transfer arguments. Additionally, airflow over a nonaqueous fluid (kerosene) was found to produce waves of higher amplitude than for water under the same conditions. These preliminary results may indicate different efficiencies of wave generation on other planets, for which empirical terrestrial relations therefore do not apply, and thus may have a bearing on the lack of strong shoreline features on Mars and the possibility of specular glints from hydrocarbon lakes on Titan.

© 2004 Elsevier Inc. All rights reserved.

**Keywords:** Mars; Titan; Geological processes; Meteorology; Experimental techniques

## 1. Introduction

The generation of waves by winds across Earth's water oceans is a topic of enduring fascination and considerable economic importance. The predictive connection between windspeed, fetch and the consequent wave-height is vital for shipping, wave energy and coastal erosion. However, the physics and mathematics of the problem are rather forbidding (e.g., Jeffreys, 1925; Stokes, 1880; Lamb, 1932; Lighthill, 1978), and consequently the relationships between real-world windspeed and sea state tend to be empirical.

Such empirical relations are of limited utility in environments where the physical parameters are different, such as the surfaces of other planets. These environments have only recently come to oceanographers' attention, with the discovery of ancient shorelines and lakes on Mars (e.g., Parker et al., 1989; Head et al., 1998), and the prospects for (e.g., Ori et al., 1998) and recent evidence of lakes and seas of liquid hydrocarbons on Saturn's moon Titan (e.g., Lorenz, 2003; Lorenz et al., 2003).

Attempts have been made to explore the possible wave characteristics on Titan since these may be observable by the recently-arrived Cassini

mission and its Huygens probe, due to descend to Titan's surface in January 2005. The Huygens probe may measure waves directly if it survives a splashdown, and sea-state may be inferred from remote observations on Cassini flybys, by measuring Sun-glint optically and/or by radar scatterometry observations.

The previous theoretical studies (e.g., Ghafoor et al., 2000) have modified empirical terrestrial wave-growth models (e.g., Komen et al., 1994; Carter, 1982) with a correction factor to account for the lower gravity. However, it is expected theoretically (e.g., Sobey, 1986; Csanady, 2001) that the energy transfer term must also include the ratio of the air and sea densities.

Because of the rather restricted range of fluid properties of interest to terrestrial oceanographers (sea-level air, water) this energy transfer term has not been studied extensively for other fluid parameters. Further, in addition to potential nonlinearity with density ratio, there is likely to be an effect of surface tension. Viscosity will also play a role, although in the dissipation terms of the energy balance. Since the momentum transfer from air to sea depends on the roughness, which in turn depends on the wave growth so far, the problem is a difficult one to solve by analytic means.

We are aware of only one other published experimental study where the fluid parameters have been varied, namely the wind-water tunnel experiments of Gottifredi and Jameson (1970). These used artificially-generated mm-scale waves at 3.8–7.6 Hz in water, glycerol solutions (higher viscosity) and surfactant solutions (lower surface tension). Lower viscosity solutions had higher wave growth rates: surprisingly, higher surface tension led to

\* Corresponding author.

E-mail address: [rlorenz@lpl.arizona.edu](mailto:rlorenz@lpl.arizona.edu) (R.D. Lorenz).

<sup>1</sup> Weber, Hayes and Associates, 120 Westgate Drive, Watsonville, CA 95076, USA.

more rapid wave growth. The liquid density was not appreciably varied and 1 bar air was used throughout.

In the present paper we report preliminary results on the early growth of capillary waves in water, the first step in the energy transfer cascade from air motion to capillary waves through to gravity waves, under an atmosphere at low pressure. This has potential application to paleo-Mars, and may help shed light on the fundamental physics of wave growth with arbitrary air and fluid properties with predictive application to Titan. Additionally, with particular relevance to Titan, we explore wave generation in a hydrocarbon liquid, with a density appreciably lower than water. These aspects have relevance for the interpretation of Cassini measurements.

## 2. Experiments

Experiments were performed in the Planetary Aeolian Facility operated by Arizona State University at NASA's Ames Research Center in Moffett Field, CA. The facility includes a  $1.2 \times 0.9 \times 13 \text{ m}^3$  working section open circuit wind tunnel that operates inside building 242 at Ames. This facility is typically used to study aeolian processes such as saltation and erosion (e.g., Bridges et al., 2004). The main part of this building, a former Titan upper stage test chamber 30 m high with a volume of some  $4000 \text{ m}^3$ , can be evacuated by steam ejector pumps, to about 3 mbar in 1 h.

For the present experiments, a fiberglass tray ( $5 \text{ cm} \times 120 \text{ cm} \times 75 \text{ cm}$ ) was installed in the tunnel, with a  $\sim 1:5$  ramp to prevent strong flow separation at the leading wall of the tray. The tray was filled to a depth of about 4 cm with tap water to which blue food coloring dye (to aid discrimination of water level in video data) had been added. Sensors were clamped to the tray itself or held by a steel and aluminium frame just above the water level. A towel was draped on the water surface at the downwind end of the tray

to act as a damper to suppress wave reflection. Figure 1 shows the tray and sensor installation in the tunnel.

Three types of sensor were used. Differential pressure sensors (OMEGA PX-139-0.3DV) with a 0–20 mbar range were used to sense the dynamic pressure above the tray as an independent record of windspeed, and to measure the varying hydrostatic head and thus the water level above one point. Position-sensitive infrared (IR) reflection sensors (Sharp GP12D02) used in mobile robotics applications were used as water level sensors—these devices using a position-sensitive detector to measure the location of a projected spot of light yield an analog voltage that is a (nonlinear) function of the distance to a reflecting surface. Finally, two ultrasonic rangefinders (Devantech DF-04), also used for mobile robotics, were installed. One was arranged vertically, like the IR sensors, to measure water level. Another sensor was canted at about  $45^\circ$  and acted as a scatterometer. The tray was observed with a video camera, whose output could be viewed on a monitor and recorded on VHS tape.

To avoid long ( $>20 \text{ m}$ ) noise-prone cable runs for the sensors, a data acquisition system was set up in the tunnel. This used a Netmedia X-24 microcontroller to strobe transmit pulses to the sonars and measure the echo time, and to perform 10-bit analog-to-digital conversion on the level and pressure sensors. These data (6 16-bit integers, and a floating-point timestamp) were transmitted on a serial link at 19200 bits per second along a coaxial cable, through a BNC feedthrough in the wall of the chamber, to the control room where they could be monitored and recorded with terminal program running on a laptop computer.

Sensor calibration was performed by incrementally filling the tray to different levels, measuring with a ruler and making a linear best fit to the sensor readings. The voltage output of the IR sensors varied as 2–3 DN/mm, while the sonar range varied as 5 DN/mm (DN refers to 'Data Numbers,' the integers reported by the X-24).

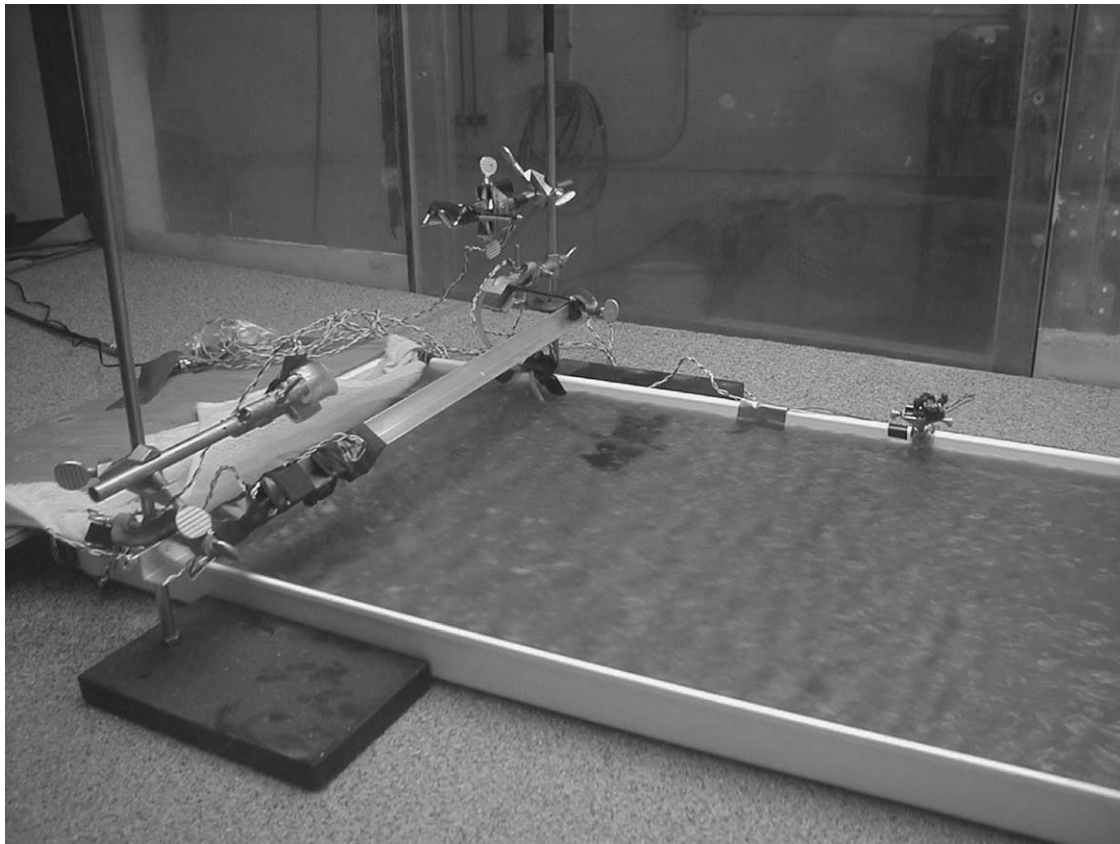


Fig. 1. Sensor installation on water tray: ripples shown for windspeed  $\sim 8 \text{ m/s}$ . Aluminum bar across tray supports the IR and sonar sensors reported in this paper (secured by black tape). The clamp immediately above has forward-canted 'scatterometer' sensor.

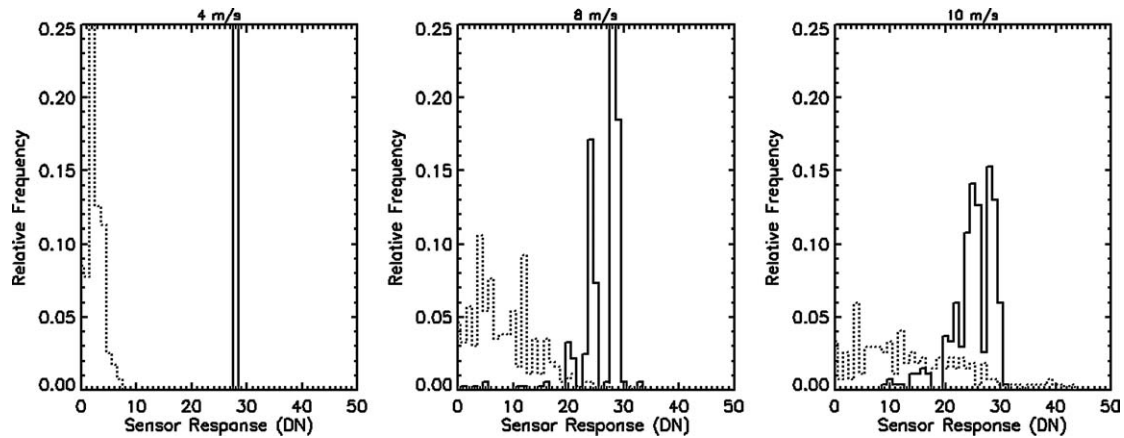


Fig. 2. Histograms of the raw sensor response (dotted line is infrared, solid line is sonar) at three different windspeeds. The sonar yields a single height at 4 m/s where waves are negligible, while the IR data have a narrow distribution due to noise. This distribution broadens as waves build up at higher windspeeds, while the sonar response bifurcates—with small waves of sinusoidal profile, the sensor responds primarily to the peaks and troughs.

### 3. Results

The wind tunnel was operated at 1 bar with experimenters present. At the lowest speed (4 m/s) only very weak shimmering of the water surface was noticed. By about 8 m/s a consistent wave pattern formed, which grew appreciably towards the maximum speed of 11 m/s.

The sensor data for the most part were consistent with this picture. The underwater pressure sensor failed to show any effects at all—evidently changes to the hydrostatic head are minimal for capillary waves. The ‘scatterometer’ sensor behaved as expected. Although quantitatively of limited utility in this investigation, the qualitative behavior was interesting—at zero speed, and at windspeeds up to 7 m/s, the sensor timed out without receiving an echo—the sound was specularly reflected away from the sensor. However, at windspeeds of 9–11 m/s, more consistent echoes were obtained—e.g., at an intermediate 8 m/s around 60% of the echoes were received. Evidently, as the windspeed and thus the surface roughness grew, returns became more and more probable.

The infrared sensors yielded good data, although only permit measurement every 30 ms, which was insufficiently fast to capture the wave shape. Furthermore, it was noted that the IR sensors over-reported the wave amplitude, due to the fact that the wave curvature distorted the perceived position of the IR reflection and thus the interpreted range to the water surface.

The ultrasound sensor detects only the reflection at the water surface: the acoustic impedance (sound speed times density) determines the reflection coefficient. The impedance for water is 3 orders of magnitude larger than that for air, so the acoustic coupling between the two is very weak and the reflection coefficient is very close to unity. The situation is less clear-cut for the IR sensor—the refractive indices of air and water are not very different, but the calibration tests showed that the sensor responded correctly at least to a flat, horizontal water surface.

The vertical sonar was perhaps the best-behaved sensor in the sense that its output statistics faithfully recovered the wave-height, confirmed by inspection of a few video images, and inspection of the histograms shown in Fig. 2. Although 60–100% of echoes were captured for pressures of 700–900 mbar, and a similar fraction for the 300 and 400 mbar runs, only between 0 and 70% of the echoes for 500–600 mbar runs were acquired; we are unable to explain this dependence. The IR data were therefore used for this pressure-sweep experiment, but the amplitudes are rescaled to the values determined for the sonar under favorable conditions.

The sonar echoes in general showed a bimodal range distribution, indicating the expected predominance of echoes from the wave crest and wave trough. We determined our ‘wave height’ as the distance spanned by the center 80% of the water surface height measurements, principally to reject noisy datapoints (the usual measure for gravity waves, ‘Significant Wave Height’ (SWH) defines the highest third of wave amplitude and is four times

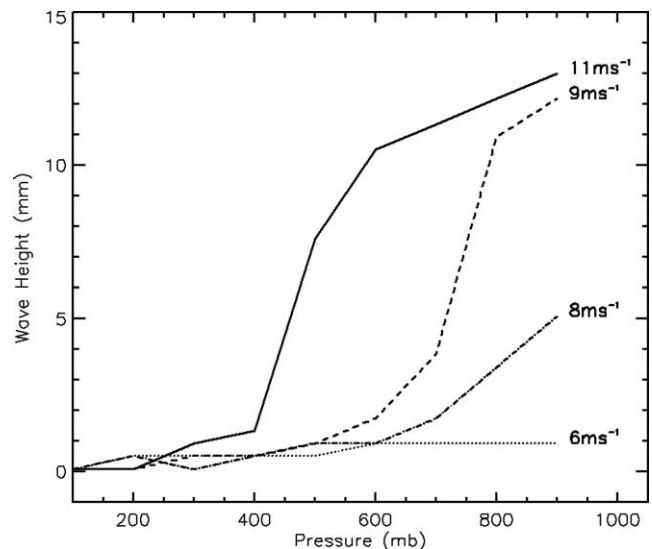


Fig. 3. Corrected IR wave amplitude for water, as a function of windspeed and ambient pressure. Larger waves occur for higher winds and higher pressure, as expected. Absolute uncertainties are of the order of 2 mm: relative errors between data points are of this order, but smaller for runs at the same pressure than between different pressures, since speed was swept at each pressure step, and pumpdown may have perturbed the setup more than simple speed adjustments.

the root variance of the sea surface height: for the purpose of this exercise, our measure is broadly comparable).

It was immediately apparent from video records, as well as casual inspection of the data, that wave generation was considerably weaker for pressures below 1 bar. The key results are summarized in Fig. 3.

While the results have certain reassuring features of consistency (e.g., 5 mm wave height occurs at a more or less constant dynamic pressure, half the product of density and windspeed squared. Since the temperature of the chamber is somewhat buffered by its thick walls, we can consider the experiment isothermal and thus density may be considered proportional to pressure: the 5 mm wave height occurs where the product of pressure and the square of windspeed is around  $50 \text{ bar m}^2/\text{s}^2$ ). The highly nonlinear dependence of wave height on surface pressure for a fixed windspeed is rather striking. Particularly notable is that wave height was insignificant compared with measurement noise for all windspeeds at pressures below about 400 mbar.

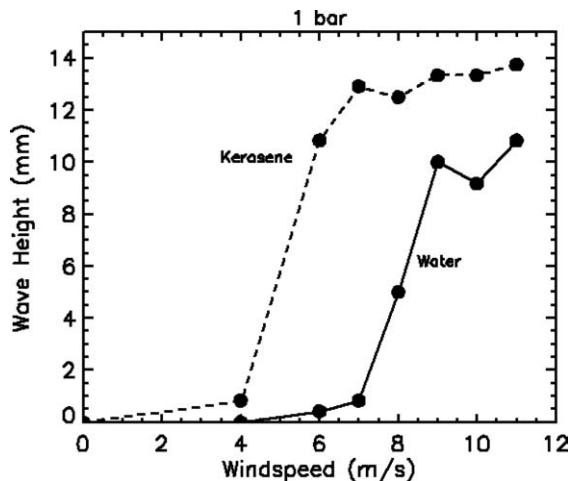


Fig. 4. Wave height for runs at 1 bar for water and for kerosene. The flattening of the curve for kerosene may indicate that wave growth in the experiment was limited by the short fetch of the tray, or its shallow depth. In any case, for the highest speeds, the height for waves in kerosene is  $\sim 25\%$  larger, and at low windspeeds waves grow much more rapidly than for water.

The threshold at 300–400 mbar, and the strong residual slope of the curves after the friction power (or rather a proxy, pressure times windspeed cubed) is divided out confirms a nonlinear dependence of wave growth on pressure, at least for the small wave heights and flow conditions of this experiment. It is unfortunately not possible to extract a drag coefficient from the data: although the wave amplitude corresponds to an energy, the rather short wave period was not resolved by the sensors, so the energy per unit time cannot be calculated.

The somewhat sigmoid shape of the curves in Figs. 3 and 4 may be due to ‘saturation’ of the waves—in the relatively shallow tray, the dissipation may grow sharply with wave amplitude. Since wave height is a dynamic equilibrium between friction (tending to increase wave height, and increasing with pressure) and dissipation (a tendency to decrease wave height, increasing with wave height) such an increase may limit the growth of waves.

#### 4. Low pressure run

Although the indications from the ‘pressure sweep’ of runs is that no observable waves were generated at 0–10 m/s windspeeds for pressures below about 400 mbar, an additional low-pressure high-speed run was performed to explore whether (very) large windspeeds could achieve wave formation even in atmospheres only just able to support liquid water. A reason for the discontinuous variation in speed from the  $\sim 10$  m/s of the previous set down to  $\sim 200$  mbar and this run at  $\sim 15$ – $30$  mbar and 35 m/s is that the fan of the wind tunnel loses performance at low pressures. At such pressures, a compressed air (9.6 bar) ejector system is used to force air through the tunnel, and this system is most effective at low tunnel pressures. (In the range 30–200 mbar neither the fan nor the compressed air are particularly effective, and speeds of only a few m/s can be realized.) At low pressure, the compressed air system should be able to achieve  $\sim 100$  m/s, but has been underperforming in recent years.

Speeds of  $\sim 35$  m/s at 15 mbar were attained—the dynamic pressure is the same as for 10 m/s at 150 mbar, but the energy dissipation rate should be close to that for 10 m/s at 450 mbar. Some small disturbances were evident via the video monitor, but many of these propagated upwind—they were caused by bubbles (of air or more likely water vapor—the boiling point of water at 15 mbar is about  $13^\circ\text{C}$ ) forming and bursting in the low pressure environment. However, no obvious wind-generated disturbances

were apparent, and within a few moments of the wind flow the surface of the water (evidently chilled by evaporation) froze over, forming ice with a thickness of  $\sim 2$  mm.

#### 5. Wave generation in nonaqueous fluids

On one day of the experiment run, when the steam plant for pumpdown was not operational, a test run was performed with the ambient atmosphere, but with a nonaqueous liquid—kerosene. This fluid was chosen for its physical properties (density  $\sim 750$  kg/m<sup>3</sup> (0.75); viscosity  $2.5 \times 10^{-4}$  Pa s (0.25) and surface tension 28 N/m (0.3), where the numbers in parenthesis indicate the ratio of those properties with respect to the values for water) which are comparable with the lighter hydrocarbons likely to form lakes and seas on Titan. Although not quite of as low density and viscosity as liquid ethane and methane at 94 K, kerosene at room temperature has the significant advantage of a sufficiently low vapor pressure as not to immediately evaporate and form an explosive gas-air mixture.

It was observed (Fig. 4) that the waves formed in kerosene for a given wind speed were larger than those formed in water. Additionally, detectable waves appear at lower speed than they did for water. It cannot be determined from this single experiment whether this is more due to the lower density or the lower surface tension, although it is notable that at the larger speeds studied, the product of wave height and density was approximately the same for both fluids.

#### 6. Conclusions and future work

The qualitative indications of these experiments can be summarized as follows: capillary wave generation appears strongly dependent on atmospheric density, and on the liquid properties. The wave height measured here is either dependent on some power ( $>1$ ) of pressure, or a threshold pressure exists below which growth simply does not occur.

The vapor pressure curve of water is such that the martian atmosphere need only be slightly denser to make seas of water thermodynamically stable—a few tens of millibar of pressure are all that are needed to prevent boiling, even with temperatures as warm as Earth (288 K average). However, some observations (e.g., Malin and Edgett, 1999; Cabrol and Grin, 1999) indicate that putative martian shorelines do not show evidence of wave erosion. While other factors such as ice cover on the seas may be responsible, the initial results here suggest that wave generation at even quite large martian pressures may have been inefficient, and thus ice-free seas may nonetheless have been present yet not form wave-cut shorelines.

We recognize that this conclusion relies upon the considerable extension of the trends we observe for cm-scale capillary waves up to large gravity waves. However, lengthy wind-wave tunnel studies with water and air (see Csanady, 2001) show that the capillary waves are instrumental in causing larger waves to grow. While no claim of proportionality or higher dependence can yet be made, it seems clear that gravity wave growth trends must follow the same direction as the capillary wave trends.

Extrapolation of the pressure trend of wave-growth with pressure to Titan conditions would favor wave-growth in its 1.5 bar atmosphere (in addition to the gravity scaling already noted in previous work—Ghafoor et al., 2000). Furthermore, our experiments show that liquid hydrocarbons grow waves more easily than does water, although the relevant parameters cannot yet be isolated. Again, this trend facilitates wave-growth on Titan. Even if the extrapolation of capillary wave-growth trends to gravity waves turns out not to be supported, the capillary wave growth for Titan is directly relevant to upcoming Cassini observations, since the Cassini RADAR has a wavelength of 2.2 cm, which is the scale of likely capillary waves on Titan (Elachi et al., 1991). The interpretation of sea-surface radar backscatter as roughness, and potentially as a diagnostic of sea-surface windspeed, therefore must take the different wave-generation efficiency in the Titan environment into account.

It is recognized that these experiments, conducted on an opportunistic basis at the Marswit facility, are far from comprehensive. They do, however, indicate a qualitatively surprising sensitivity of wave growth to atmospheric density, and a significant influence of liquid properties. A more systematic evaluation of the wave growth under various parameters is therefore advocated. Such an investigation would benefit from faster-sampled wave-profile sensors, a longer and deeper tray, ancillary measurements including flow visualization to confirm smooth airflow over the liquid surface, and a broader selection of liquid properties.

### Acknowledgments

The Mars Surface Wind Tunnel (MARSWIT) is operated by Arizona State University's Department of Geological Sciences at NASA Ames Research Center in Moffett Field, CA, with support from the NASA Planetary Geology and Geophysics Program. R.L. acknowledges support of the Cassini project. E.K. is supported by a NASA Graduate Student Research Program award. The authors thank Erik Asphaug, Jeff Moore, and Steve Saunders for encouraging these preliminary experiments. We thank two anonymous referees for useful comments.

### References

- Bridges, N.T., Laity, J.E., Greeley, R., Phoreman, J., Eddlemon, E.E., 2004. Insights on rock abrasion and ventifact formation from laboratory and field analog studies with applications to Mars. *Planet. Space Sci.* 52 (1-3), 199-213.
- Cabrol, N.A., Grin, E.A., 1999. Distribution, classification, and ages of martian impact crater lakes. *Icarus* 142, 160-172.
- Carter, D.J.T., 1982. Predictions of wave height and period for a constant wind velocity using the JONSWAP results. *Ocean Eng.* 9 (1), 17-33.
- Csanady, G.T., 2001. *Air-Sea Interaction: Laws and Mechanisms*. Cambridge Univ. Press, New York.
- Elachi, C., Im, E., Roth, L.E., Werner, C.L., 1991. Cassini Titan radar mapper. *Proc. IEEE* 79, 867-880.
- Ghafoor, N., Zarnecki, J.C., Challenor, P., Srokosz, M.A., 2000. Wind-driven waves on Titan. *J. Geophys. Res.* 105 (E5), 12077-12091.
- Gottifredi, J.C., Jameson, G.J., 1970. The Growth of short waves on liquid surfaces under the action of a wind. *Proc. R. Soc. Ser. A* 319, 373-397.
- Head III, J.W., Kreslavsky, M., Hiesinger, H., Ivanov, M., Pratt, S., Seibert, N., Smith, D.E., Zuber, M.T., 1998. Oceans in the past history of Mars: tests for their presence using Mars Orbiter Laser Altimeter (MOLA) data. *Geophys. Res. Lett.* 25, 4401-4404.
- Jeffreys, H., 1925. On the formation of water waves by wind. *Proc. R. Soc. Ser. A* 107, 189-207.
- Komen, G.J., Cavaleri, L., Donelan, M., Hasselmann, K., Hasselmann, S., Janssen, P.A.E.M., 1994. *Dynamics and Modelling of Ocean Waves*. Cambridge Univ. Press, New York.
- Lamb, H., 1932. *Hydrodynamics*, sixth ed. Dover, New York.
- Lighthill, J., 1978. *Waves in Fluids*. Cambridge Univ. Press, New York.
- Lorenz, R.D., 2003. The glitter of distant seas. *Science* 302, 403-404.
- Lorenz, R.D., Kraal, E., Asphaug, E., Thomson, R., 2003. The seas of Titan. *EOS* 84 (14), 125-132.
- Malin, M.C., Edgett, K.S., 1999. Oceans or seas in the martian northern lowlands: high-resolution imaging tests of proposed coastlines. *Geophys. Res. Lett.* 26 (19), 3049-3053.
- Ori, G.G., Marinangeli, G., Baliva, L., Bressan, A., Strom, R., 1998. Fluid dynamics of liquids on Titan's surface. *Planet. Space Sci.* 46 (9/10), 1417-1421.
- Parker, T.J., Saunders, R.S., Schneeberger, D.M., 1989. Transitional morphology in west Deuteronilus Mensae, Mars. Implications for modification of the lowland/upland boundary. *Icarus* 82, 111-145.
- Sobey, R.J., 1986. Wind-wave prediction. *Annu. Rev. Fluid. Mech.* 18, 149-172.
- Stokes, G.G., 1880. Considerations relative to the greatest height of oscillatory irrotational waves which can be propagated without change of form. *Math. Phys. Papers* 1 (1), 225-228.